

STAFF SUMMARY SHEET

	TO	ACTION	SIGNATURE (Surname), GRADE AND DATE		TO	ACTION	SIGNATURE (Surname), GRADE AND DATE
1	DFP	sig	<i>Anderson O.S, 2 MAR 15</i>	6			
2	DFER	approve	<i>SOLTE, AD25, 2 MAR 15</i>	7			
3	DFP	action		8			
4				9			
5				10			

SURNAME OF ACTION OFFICER AND GRADE	SYMBOL	PHONE	TYPIST'S INITIALS	SUSPENSE DATE
Balthazor, CTR	DFP	333-4231	rlb	—

SUBJECT	DATE
Clearance for Material for Public Release	USAFA-DF-PA-037

SUMMARY

1. **PURPOSE.** To provide security and policy review on the document at Tab 1 prior to release to the public.

2. **BACKGROUND.**
 Authors: Balthazor, R.L. (DFP, 333-4231), McHarg, M.G. (DFP, 333-2460), Enloe, C.L. (DFP, 333-2240), Mueller, B.A.(former DFP cadet), Barnhart, D.J. (DFAS, 333-3315), Hoeffner, Z. (former DFP cadet), Brown, R. (DFAS, 333-4454), Scherliess, L.(Utah State University, 435 797 7189), and Wilhelm, L. T. (former DFP cadet)

Title: Methodology Of Evaluating The Science Benefit Of Various Satellite/Sensor Constellation Orbital Parameters To An Assimilative Data Forecast Model.

Document type: Paper

Description: This is a paper to be submitted to a special issue of the journal Radio Science.

Release Information: General overview good for all audiences

Previous Clearance information: The paper's initial submission has previous been cleared as DFP submissions 14010 and 14048. This submission has been amended/ revised to answer yet more points raised by reviewers.

Recommended Distribution Statement: Distribution A, Approved for public release, distribution unlimited.

3. **DISCUSSION.** This research is funded by AFOSR and the NSF.

4. **VIEWS OF OTHERS.** N/A

5. **RECOMMENDATION.** Sign coord block above indicating document is suitable for public release. Suitability is based solely on the document being unclassified, not jeopardizing DoD interests, and accurately portraying official policy.

// signed //

MONTE D. ANDERSON, Lt Col, USAF
 Deputy Department Head for Research
 Department of Physics

Tabs
 1. Paper transcript

STAFF SUMMARY SHEET

	TO	ACTION	SIGNATURE (Surname), GRADE AND DATE		TO	ACTION	SIGNATURE (Surname), GRADE AND DATE
1	DFP	sig	<i>Anderson O.S, 2 MAR 15</i>	6			
2	DFER	approve	<i>SOLTE, AD25, 2 MAR 15</i>	7			
3	DFP	action		8			
4				9			
5				10			

SURNAME OF ACTION OFFICER AND GRADE	SYMBOL	PHONE	TYPIST'S INITIALS	SUSPENSE DATE
Balthazor, CTR	DFP	333-4231	rlb	—

SUBJECT	DATE
Clearance for Material for Public Release	USAFA-DF-PA-037

SUMMARY

1. **PURPOSE.** To provide security and policy review on the document at Tab 1 prior to release to the public.

2. **BACKGROUND.**
 Authors: Balthazor, R.L. (DFP, 333-4231), McHarg, M.G. (DFP, 333-2460), Enloe, C.L. (DFP, 333-2240), Mueller, B.A. (former DFP cadet), Barnhart, D.J. (DFAS, 333-3315), Hoeffner, Z. (former DFP cadet), Brown, R. (DFAS, 333-4454), Scherliess, L. (Utah State University, 435 797 7189), and Wilhelm, L. T. (former DFP cadet)

Title: Methodology Of Evaluating The Science Benefit Of Various Satellite/Sensor Constellation Orbital Parameters To An Assimilative Data Forecast Model.

Document type: Paper

Description: This is a paper to be submitted to a special issue of the journal Radio Science.

Release Information: General overview good for all audiences

Previous Clearance information: The paper's initial submission has previous been cleared as DFP submissions 14010 and 14048. This submission has been amended/revised to answer yet more points raised by reviewers.

Recommended Distribution Statement: Distribution A, Approved for public release, distribution unlimited.

3. **DISCUSSION.** This research is funded by AFOSR and the NSF.

4. **VIEWS OF OTHERS.** N/A

5. **RECOMMENDATION.** Sign coord block above indicating document is suitable for public release. Suitability is based solely on the document being unclassified, not jeopardizing DoD interests, and accurately portraying official policy.

// signed //

MONTE D. ANDERSON, Lt Col, USAF
 Deputy Department Head for Research
 Department of Physics

Tabs
 1. Paper transcript

1

2 **Methodology of evaluating the science benefit of various satellite/sensor constellation**
3 **orbital parameters to an assimilative data forecast model.**

4 Richard L. Balthazor, Matthew G. McHarg, C. Lon Enloe, Brandon Mueller, David J. Barnhart,
5 Zachary W. Hoeffner, and Robert Brown, United States Air Force Academy, Colorado, USA.

6 Ludger Scherliess, Center for Atmospheric and Space Sciences, Utah State University, Logan,
7 Utah, USA.

8 Lance T. Wilhelm, Air Force Research Laboratory, AFRL/RXCA, Dayton, Ohio, USA

9

10 Corresponding author: R. L. Balthazor, Space Physics and Atmospheric Research Center, HQ
11 USAFA/DFP, 2354 Fairchild Drive, USAF Academy, CO 80840, USA
12 (richard.balthazor@usafa.edu)

13

14

15 **Key Points**

16 Methodology for evaluating benefit of increasing assimilative data sources

17

18 **Abstract**

19 A methodology for evaluating the science benefit of adding space weather sensor data from a
20 modest number of small satellites to the Utah State University Global Assimilation of
21 Ionospheric Measurements – Full Physics (GAIM-FP) model is presented. Three orbital
22 scenarios are presented, two focusing on improved coverage of narrowly specified regions of
23 interest, and one on global coverage of the ionosphere as a whole. An Observing System
24 Simulation Experiment (OSSE) is used to obtain qualitative and quantitative results of the impact
25 of the various orbital scenarios on the ionospheric specifications. A simulated “truth” run of the
26 ionosphere is obtained from a first principles model of the Ionosphere/Plasmasphere model
27 (IPM) and used to generate global simulated Global Positioning Satellite Total Electron Content
28 (GPS-TEC) data as well as in-situ plasma density observations. Initially, only GPS data were
29 assimilated by GAIM-FP and the results of this limited run were compared to the truth run. Next,
30 the simulated in-situ plasma densities corresponding to our three orbital scenarios were
31 assimilated together with the GPS data and the results were compared to both the truth run and
32 the limited GPS-TEC only GAIM-FP run. These model simulations have shown that adding a
33 constellation of small satellites/sensors in addition to global TEC inputs does indeed converge
34 the GAIM-FP model closer to “truth” in the situations described.

40

41 1. Introduction

42 In recent years, there have been constructed or proposed space sensor networks [Anderson et al,
43 2002; Barnhart et al, 2007a, 2007b; Barnhart, 2008; Barnhart et al, 2009; Vladimirova et al,
44 2011; Dyrud et al, 2013] designed to cover selected orbits in LEO with either:

- 45 i) low-cost redundant “disposable” spacecraft-as-sensor platforms of CubeSat 3U size or
46 smaller, or
- 47 ii) low-cost low-SWAP (Size, Weight and Power) sensors designed to be placed on as many
48 conventional (ESPA-class or larger) satellites as possible.

49 The science objective of many of these missions is to provide a dense set of sensor data
50 parameters to “fill in the gaps” of the relatively sparse coverage afforded by conventional multi-
51 million-dollar missions [de la Beaujardiere, 2004] which produce single-point in-situ or remote
52 measurements.

53 Despite the lower cost of small satellites and low-SWAP instrumentation, limitations include
54 funding, choice of orbital parameters in launch opportunities, space debris mitigation, and data
55 volume/bandwidth consideration. A key question asked by funders and approvers is still “how
56 many satellites/sensors are enough?” What has become apparent is that there is no generally
57 agreed metric for determining the scientific justification side of this argument, and we propose
58 one methodology to obtain quantitative metrics, which may assist in answering that question.

59

60 2. Scientific Problem and Background

61 The science problem that we identify for this study is space weather forecasting, particularly
62 forecasting of plasma irregularities (“plasma bubbles”) that cause radio and GPS scintillation.
63 Such scintillation can cause loss of GPS lock (less than 50% availability for LPV-200 during
64 severe scintillation [Seo, 2010]), loss of communications, and image defocussing in synthetic
65 aperture radar. (LPV stands for Localizer Performance with Vertical Guidance. It refers to a
66 precision approach system for aviation. LPV-200 availability indicates the probability for a GPS-
67 autopilot-equipped plane to reach a 200’ decision height (the height at which the pilot has to
68 make the land/go-around decision and assume manual control). It is one metric used to determine
69 the efficacy of GPS locational ability.) Forecasting (and nowcasting) ionospheric conditions
70 conducive to plasma bubble formation would therefore seem to require global assimilative
71 models of the ionosphere to provide baseline conditions in the regions of interest, and it is on this
72 facet that we concentrate.

73 Our ability to specify and forecast ionospheric dynamics and ionospheric weather at low and mid
74 latitudes is strongly limited by our current understanding of the coupling processes in the
75 ionosphere-thermosphere system and the coupling between the high and low latitude regions.
76 Furthermore, only a limited number of observations are available for a specification of
77 ionospheric dynamics and ionospheric weather at these latitudes. As shown by meteorologists
78 and oceanographers, the best specification and weather models are physics-based data
79 assimilation models that combine the observational data with our understanding of the physics of
80 the environment [Daley, 1991]. Through simulation experiments these models can also be used
81 to study the sensitivity of the specification accuracy on different arrangements of observation

82 platforms and observation geometries and can provide important information for the planning of
83 future missions. For example, these studies can provide information about the number of
84 spacecraft needed to improve the specification or evaluate the impact of different observation
85 geometries on the accuracy of the specification.

86 **3. Instrument and Satellite Concept**

87 Previous efforts in flying low-cost space weather instruments have focused on low-impact
88 secondary payloads riding on larger (e.g. ESPA-class) satellites. These have advantages, in that
89 the larger satellites tend to be more reliable (through extensive heritage and testing) and have
90 larger link budgets and power margins. However, there are higher integration costs (particularly
91 when co-riding with high-value primary payloads), longer project timescales, and more
92 expensive busses (\$10M+). They also provide only a few in-situ measurements for each satellite,
93 and have relatively long delays before resampling the same dataspace.

94 There have, however, been recent advances in thinking regarding multiple low-cost redundant
95 satellites carrying low-cost sensors. Such a large constellation has many applications; treaty
96 sentinels, disaster monitoring, magnetospheric observations, solar wind measurements, pollution
97 monitoring and communications research to name but a few. In many of the above cases we
98 currently undersample the data field. We concentrate our approach for this paper on the
99 thermosphere/ionosphere system, ingesting plasma density and temperature data from in-situ
100 measurements into an assimilative model, although the general methodology is applicable to any
101 of the above applications.

102 With this approach there are a number of suitable instruments with low SWAP that obtain in-situ
103 ionospheric parameters (we restrict ourselves to in-situ measurements for this study, although a
104 similar methodology may be used with remote measurements). The MESA (Miniaturized
105 ElectroStatic Analyzer) instrument [Enloe et al, 2002] is a bandpass or high-pass energy filter (in
106 either of two configurations). The instrument thus measures ion or electron spectra (convolved
107 with the instrument response function) from which plasma density and temperature can be
108 derived. MESAs have flown on MISSE-6, MISSE-7 [Jenkins et al, 2009], ANDE-2,
109 FalconSAT-5, STP-H4 and STPSat-3, and are rostered to fly on OTB and other missions.
110 Another instrument of interest is WINCS (Winds Ions Neutrals Composition Suite) and its sister
111 instrument SWATS (Small Wind And Temperature Spectrometer), developed by the Naval
112 Research Laboratory. WINCS and SWATS are sensor suites measuring ion and neutral winds,
113 temperature and composition (<http://www.nrl.navy.mil/ssd/branches/7630/SWATS>). More
114 generic/traditional Langmuir probes and Retarding Potential Analyzers are also instruments that
115 may with care be integrated into a low SWAP package (although the standoff length of a
116 Langmuir probe may prove to be challenging).

117

118 **4. GAIM-FP Comparison Methodology**

119 At Utah State University, we have developed two physics-based Kalman-filter data assimilation
120 models for the Earth ionosphere. The two models are the Gauss-Markov Kalman Filter Model
121 (GAIM-GM) and the Full Physics-Based Kalman Filter Model (GAIM-FP) [Scherliess et al.,
122 2006, 2009]. Both models are part of the Global Assimilation of Ionospheric Measurements
123 (GAIM) project [Schunk et al. 2004]. Some of the data that we have previously assimilated in

124 our data assimilation models include in-situ electron density measurements from DMSP
125 satellites, bottomside electron density profiles from ionosondes, GPS-TEC data from a network
126 of up to 1000 ground stations, ultraviolet (UV) radiances from the SSUSI (Special Sensor
127 Ultraviolet Spectrographic Imager), SSULI (Special Sensor Ultraviolet Limb Imager), and
128 LORAAS (Low Resolution Airglow and Aurora Spectrograph) instruments, and radio
129 occultation data from CHAMP (Challenging Minisatellite Payload), SAC-C (Satellite de
130 Aplicaciones Cientificas-C) [Hajj *et al.*, 2004], IOX (Ionospheric Occultation Experiment)
131 [Straus *et al.*, 2003], and the COSMIC (Constellation Observing System for Meteorology,
132 Ionosphere and Climate) [Rocken *et al.*, 2000] satellites.

133 The Full Physics-Based Kalman filter model is based on an ensemble Kalman filter approach
134 [Evensen, 2003] and rigorously evolves the ionosphere and plasmasphere electron density field
135 and its associated errors using a physics-based Ionosphere-Plasmasphere model (IPM) [Schunk *et*
136 *al.*, 2004, 2005; Scherliess *et al.*, 2004]. The IPM is based on a numerical solution of the ion and
137 electron continuity and momentum equations and covers the low and mid-latitudes from 90 to
138 30,000 km altitude. In its current version, the model excludes geomagnetic latitudes poleward of
139 $\approx \pm 60^\circ$ geomagnetic latitude due to the vastly different physical processes that govern the high-
140 latitude regions, e.g. convection electric fields, particle precipitation, etc. The Full Physics-Based
141 data assimilation model provides specifications on a spatial grid that can be global, regional, or
142 local and its output includes the 3-dimensional electron and ion (NO^+ , O_2^+ , N_2^+ , O^+ , H^+ , He^+)
143 density distributions from 90 km to near-geosynchronous altitude (30,000 km). In addition, the
144 model provides the global distribution of the ionospheric drivers (electric field, neutral wind, and
145 composition) that make the modeled state consistent with the ionospheric observations. It is
146 important to note that the estimation of the ionospheric drivers is an integral part of our ensemble

147 Kalman filter and is achieved by using the internal physics-based model sensitivities to the
148 various driving forces. In this procedure, the ionospheric data are used to adjust the plasma
149 densities and its drivers so that a consistency between the observations (within their errors) and
150 the physical model is achieved. As a result the assimilation procedure produces the optimal
151 model-data combination of the ionosphere-plasmasphere system together with the set of drivers
152 (electric fields and neutral winds and composition) consistent with the ionospheric observations
153 [Scherliess *et al.*, 2009, 2011].

154 **4.1 Kalman Filter Simulations**

155 The Full Physics-Based data assimilation model was designed to specify ionospheric weather,
156 but the model can also be used to study the sensitivity of the specification accuracy on different
157 arrangements of observation platforms and observation geometries and can provide important
158 information for the planning of future missions [e.g. *Atlas*, 1997; *Atlas et al.*, 1985]. For the
159 current study this latter mode has been used and simulation experiments have been performed. In
160 this mode the model uses an Observing System Simulation Experiment (OSSE) using two
161 different synthetic (model-generated) data types: slant TEC from ground-based GPS stations and
162 in-situ plasma density measurements obtained from electrostatic analyzers (ESA) onboard of a
163 constellation of small satellites. Figure 1 shows a snapshot of the geographic distribution of
164 ground-based GPS-TEC observations shown at their 300 km pierce points used in this study. In
165 the OSSE, the simulated weather (true) time-dependent ion and electron density distributions are
166 generated by using again the IPM model. For this study we have used two geomagnetically quiet
167 days, 2010 day 73 and 74 (March 14th/15th) where Kp=1 throughout the two days. These two
168 days were chosen to assist in another study comparing actual MESA data from the MISSE7

169 experiment on the ISS with the GAIM predictions; that work is outside the scope of this paper.
170 However, for the purposes of this paper discussing the application of a proposed methodology,
171 these days may be considered arbitrary; we are not attempting to arrive at an absolute “truth”
172 measurement for these days in this paper, but rather apply a general methodology applicable
173 regardless of the days selected (within the applicable range of geomagnetic conditions of the
174 assimilative model used), the satellite constellation orbital parameters, the specific
175 characteristics/precision/accuracy of the sensor/instrument suite used, other data sources ingested
176 into GAIM, etc.

177 For the simulations we varied the equatorial vertical drift and horizontal neutral winds by
178 superposing on the climatology values a random component. At low and middle latitudes, the
179 important inputs into the IPM are the neutral wind field and the equatorial electric field. The
180 empirical horizontal wind model (HWM) was used to generate the neutral wind field and the
181 empirical Scherliess-Fejer equatorial vertical drift model was used for the equatorial electric
182 fields. When these empirical inputs are used, the IPM yields ionospheric climatology that is
183 consistent with the empirical inputs. The goal of the present study is however not to reproduce
184 climatology, but to reproduce real-time weather features. Consequently, a disturbed ionosphere
185 that represents weather is needed for the OSSE. The disturbed ionosphere was obtained by
186 adding to the climatological neutral wind and electric field values a random component at each
187 15-minute time step. For the electric fields (vertical drifts) a random value between ± 10 m/s was
188 chosen and for the neutral wind a random value of ± 50 m/s was chosen. This IPM run was
189 assumed to represent weather and was taken to be the truth. Clearly, there are a couple of
190 important caveats associated with these model runs. For example the truth run only varied the
191 neutral wind and low latitude electric fields and did not, for example, considered changes in the

192 temperatures and other ionospheric/thermospheric parameters. Note that neither the
193 climatological values nor the random components are known to the ensemble Kalman filter part.

194 The synthetic data were then generated by probing the 3-D, time-dependent electron density
195 distribution for the weather (true) simulation exactly the same way the real instruments probe the
196 real ionosphere. For the GPS receivers, slant TEC values were generated only for elevation
197 angles greater than 15°. For the in-situ electron densities synthetic observations were generated
198 in 10-sec increments. When the synthetic data were generated, noise was added to each
199 “measurement” in order to mimic a real observation. A 5 TEC unit (TECU) level of noise was
200 added to all simulated TEC measurements and a 10% uncertainty to the simulated in-situ
201 measurements. It should be noted that the 10 second resolution of the observations is not
202 intended to capture variations that occur on this small time step, but instead to capture spatial
203 variations of the order of about 100-150 km around the latitudinal resolution of the model. 10
204 seconds is also the nominal cadence of data-taking in the IMESA instrument (although it is
205 capable of running as fast as 2Hz). The satellites traverse a distance of about 70 km in 10
206 seconds, which provides about two observations per latitude grid cell. The model time step of 15
207 minutes was chosen to capture typical variations in the ionospheric F-region where the
208 characteristic timescales are of the order of tens of minutes.

209 The ensemble Kalman filter assimilation procedure was implemented as follows. At 0000 UT on
210 day 2010/073 the plasma distribution obtained from the “truth” run (the IPM run with the
211 modified climatological neutral wind and equatorial electric field input) was taken to be the
212 initial distribution at the start of the assimilation. Every 15 min, the evolving weather simulation
213 was probed to obtain the two synthetic data types (with noise) as described above. At these time

214 marks the ensemble of ionosphere/plasmasphere model runs was also integrated forward in time,
215 and the model error covariance matrix was determined [Scherliess *et al.*, 2007]. Using the new
216 data and the new error matrix, the ensemble Kalman filter reconstructed an updated estimate of
217 the plasma distribution and its drivers. The new drift and wind velocities were fed back into the
218 IPM and the assimilation was repeated at the next 15 min time mark. As time advanced, the
219 ensemble Kalman filter produced an estimation of the 3-D, time-dependent, plasma distribution
220 from low- to mid-latitudes.

221 To qualitatively and quantitatively assess the impact of the MESA observations on the plasma
222 specifications four ensemble Kalman filter simulations were performed. Initially, the GAIM-FP
223 model assimilated only the simulated global TEC data to obtain a specification of the plasma
224 density for the two days. This model simulation is referred to as the “ionospheric specification”
225 and may be compared with the “truth” measurement to determine the accuracy of the data
226 assimilation model.

227 Note, that neither the climatological neutral wind or the equatorial electric fields nor the imposed
228 random variations added to them are known to the filter in advance. The reason for this choice is
229 that on any given day the empirical climatology values can be far off from the actual values for
230 this day. The filter instead starts from a zero value for both the drifts and neutral winds and
231 estimates the required values for the given day. With this, the filter would not have had good
232 convergence if no data would have been assimilated.

233 Next, the synthetic MESA “observation”, including an observational uncertainty, were
234 assimilated together with the synthetic global TEC data to simulate data-taking from satellite
235 constellations that did not, in reality, exist at that particular time. The simulated observations

236 were taken along satellite tracks for three different orbital scenarios at 10 second simulated
237 cadence. The orbital scenarios were chosen to give both low-cost (single launch) rapid re-
238 coverage of a localized area, and higher-cost (multiple launches) global coverage. We also
239 wished to investigate effect of varying the altitude of the satellites on the sensitivity of the
240 specification. Accordingly, the three orbital scenarios chosen were as follows:

241 Scenario A: Ten satellites in a circular 500 km altitude polar orbit (90° inclination). Small
242 (deliberate) variations in the satellite surface treatment will lead to small variations in
243 satellite drag, causing the satellites to distribute themselves along the orbital path until they
244 are spread evenly along the orbit. This represents the “string of pearls” configuration for a
245 single launch/deployment.

246 Scenario B: As scenario A, but at a 350 km altitude.

247 Scenario C: A 25/5/1 Walker constellation at 510 km altitude and 60° inclination. The
248 Walker constellation notation of $t/p/f$ [Wertz, 2006] designates t satellites arranged over p
249 evenly spaced orbital planes (circular orbits) with f relative spacing between satellites in
250 adjacent planes. Thus, a 25/5/1 constellation has 25 satellites, five satellites per orbital plane.
251 We have picked a nominal relative spacing in this instance. This would generally require five
252 launch vehicles, each deploying five satellites, with each group deploying into the string of
253 pearls configuration after some weeks. Figure 2 shows (lower panel) Ne at 510 km, and
254 (upper panel) the ground tracks of a 25/5/1 Walker constellation with the color scale along
255 each ground track demonstrating the sampling of Ne.

256 For each of the three orbital scenarios the GAIM-FP model was used together with the global
257 TEC inputs and the MESA “observation” to obtain another set of specifications of the same day.
258 These model simulations are referred to as the “improved ionospheric specification”, and may be
259 compared to the original “ionospheric specification” (without any MESA data inputs) and the
260 original “truth” model run.

261 **5. Results**

262 For Scenarios A and B, we have examined a vertical slice of the ionosphere from 100 km to 600
263 km altitude along the 161.25° E line of longitude of the orbital plane, stretching from 60° N to
264 60° S. (Plots are plotted to the poles, but the GAIM model used only extends to $\pm 60^\circ$ magnetic
265 latitude). Figure 3 shows the deviation from “truth” in units of ΔN_e (cm^{-3}) for three simulation
266 runs: “ionospheric specification” using only GPS-TEC inputs to the assimilative forecast model
267 (left panel), “improved ionospheric specification” using GPS-TEC inputs plus inputs from
268 satellites in scenario A (center panel) (satellites at 500 km), and “improved ionospheric
269 specification” using GPS-TEC inputs plus inputs from satellites in scenario B (right panel)
270 (satellites at 350 km).

271 A visual inspection of the data shows that utilizing inputs from a modest constellation of ten
272 satellites at either of two altitudes shows a distinct improvement to the “improved ionospheric
273 specification” (ΔN_e converges towards zero). What is perhaps remarkable is that the
274 improvement is distinct at most latitudes and can be seen at all altitudes and not just at the orbital
275 altitude. The apparent propagation of information to other altitude regimes is very likely a
276 manifestation of the strong correlation of electron density variations along geomagnetic field
277 lines. These correlations are part of the ensemble Kalman filter and automatically calculated

278 using the ensemble of physics-based model runs. This indicates that the useful life of such a
279 constellation, as orbital drag decays the orbit from the initial insertion, will be extended through
280 the life of the mission (months to years for higher initial orbital insertions), rather than losing
281 their use after initial orbital decay.

282 Scenario C allows inspection of global (latitude-longitude) coverage. We have elected to use
283 hmF2 as a proxy for our knowledge of the ionosphere (remembering that although the satellites
284 in Scenario C are at 500 km, the earlier results indicate that information is apparently
285 propagating vertically (most likely associated with the correlation of electron density along
286 magnetic field lines in the ensemble Kalman filter) allowing us to inspect the ionosphere and the
287 improvement to the plasma specifications at any altitude). We inspect hmF2 at an arbitrary time
288 of 1600 GMT on day 2010/073. Figure 4 shows hmF2 from the “truth” model (plotted to the
289 latitude limits of the model) at the selected time. Figure 5 shows hmF2 obtained from the
290 “ionospheric specification” model using only GPS-TEC inputs to the model. A visual inspection
291 shows that there are deviations from “truth”. In particular, the height enhancement over the
292 Japanese sector is not found; there is an erroneous equatorial plume forecast over the Indonesian
293 sector; and the pronounced equatorial anomaly over the South American sector is not seen in the
294 data assimilation results for this limited model run.

295 Figure 6 shows hmF2 obtained from the “improved ionospheric specification”, utilizing GPS-
296 TEC inputs plus simulated data from the MESA instruments in the Walker constellation of
297 scenario C. Inspection shows that the three features mentioned above, reproduced poorly by the
298 “ionospheric specification”, are present in the “improved ionospheric specification”.

299 The previous examples are qualitative. There are many quantitative metrics that can be used to
300 quantify the improvement, and we have arbitrarily selected two metrics, the RMS deviation
301 (global sum) and the Skill Score (global sum). The RMS deviation, summed over all latitude-
302 longitude points at each hmF2 altitude, is given by the sum of the squares of the deviations from
303 truth divided by the number of observations and is measured in km (equation 1). Improved
304 modeling will reduce the RMS deviation towards zero.

305 The Skill Score is a measure of improvement of one model over another and is unitless, ranging
306 from $-\infty$ to +1. If the second model is perfect the Skill Score tends to +1, and if the second
307 model predicts no better than random chance the Skill Score tends towards 0 (equation 2).

$$308 \quad RMS = \sqrt{\frac{\sum(Truth - Obs)^2}{N}} \quad (1)$$

$$309 \quad Skill\ Score = 1 - \frac{\sum(Truth - (GPS+IMESA))^2}{\sum(Truth - GPS\ only)^2} \quad (2)$$

310 Figure 7 shows the RMS deviation from truth global sum over a 24-hour period on 2010 day
311 073. With the “ionospheric specification” (GPS-TEC only), the RMS deviation from truth varies
312 between 25 km and 100 km over the course of the 24 hours. It is interesting to note the variation
313 over time, and we suggest that this is due a function of daytime and nighttime regions being
314 densely or less densely populated with GPS-TEC ground stations, as the sun moves from the
315 Pacific sector (less densely populated with GPS-TEC ground stations) to the American and
316 European sectors (more densely populated). With the “improved ionospheric specification”
317 (GPS-TEC plus simulated MESA data from scenario C), which of course are agnostic to day-

318 night variations, the RMS deviation global sum improves to around 10 km over the course of the
319 day.

320 The Skill Score comparison of the two model runs is shown in Figure 8. Again we see a
321 pronounced diurnal response, with the “improved ionospheric specification” performing
322 extremely well in the 0000 UT to 0600 UT, and 1800 UT to 2359 UT timeframes, and
323 marginally less well between those timeframes. However, with the Skill Score minimum being
324 -0.75 , we can conclude that overall there is a marked improvement to our forecast model with 25
325 MESAs in orbital scenario C.

326 We recognize that the results obtained from these metrics can depend on other parameters such
327 as geomagnetic activity, but such an investigation is outside the bounds of this paper.

328 **6. Conclusions**

329 We have proposed using a simple sensor that measures ion and electron energy spectra, from
330 which plasma density and temperature can be derived, in a low-cost mission of small
331 satellites/sensors. A full physics ionospheric model has been utilized to derive “truth” data. The
332 GAIM-FP data assimilation model has then been run both without and with simulated sensor
333 data inputs. Our model simulations have shown that adding a constellation of small
334 satellites/sensors in addition to global TEC inputs converges the GAIM-FP model closer to
335 “truth” in the situations we describe. For a real-life mission for which a launch has not been
336 imposed, a desired improvement metric may be selected and thus orbital parameters can be fine-
337 tuned to optimize the model improvement for the metric of interest. What is particularly
338 interesting is that the model is improved over a range of altitudes, not just at and around the

339 satellite/sensor altitude, emphasizing the coupled nature of both the model and reality. Put
340 another way, knowledge at one location leads to improved knowledge at other locations.

341 However, what has become apparent is the challenge to develop a generally agreed metric or set
342 of metrics to measure the scientific and operational benefit to assimilative models from the use
343 of multiple small satellite/sensor inputs.

344 **7. Acknowledgements**

345 The GAIM-FP data is publicly available on request from USU, POC Ludger Scherliess,
346 ludger.scherliess@usu.edu

347 The authors wish to thank the Air Force Office of Scientific Research for their support.

348 The work at Utah State University was partially supported by NSF grant AGS-1329544.

349

350 **8. References**

351 Anderson, B. J., Takahashi, K., Kamei, T., Waters, C. L., & Toth, B. A. (2002). Birkeland
352 current system key parameters derived from Iridium observations: Method and initial validation
353 results. *Journal of Geophysical Research: Space Physics (1978–2012)*, 107(A6), SMP-11.

354 Atlas, R. (1997) Atmospheric observations and experiments to assess their usefulness in data
355 assimilation. *JMSJ*, Vol. 75, pp. 111-130.

356 Atlas, R., E., Kalnay, J. Susskind, W. E. Baker and M. Halem (1985): Simulation studies of the
357 impact of future observing systems on weather prediction. Proc. Seventh Conf. on NWP. 145-
358 151.

359 Barnhart, D. J., T. Vladimirova, M. N. Sweeting, R. L. Balthazor, C. L. Enloe, L. H. Krause, T.
360 J. Lawrence, M. G. Mcharg, J. C. Lyke, J. J. White, and A. M. Baker (2007), Enabling Space
361 Sensor Networks with PCBSat, AIAA Paper SSC07-IV-4.

362 Barnhart, D. J., T. Vladimirova, and M. N. Sweeting, (2007), Very Small Satellite Design for
363 Distributed Space Missions, *Journal of Spacecraft and Rockets*, Vol. 44, No. 6, pp. 1294-1306.

364 Barnhart, D. J. (2008), Very Small Satellites Design for Space Sensor Networks, Ph.D. Thesis,
365 Univ. of Surrey, Guildford, England, U.K., <http://handle.dtic.mil/100.2/ADA486188>.

366 Barnhart, D.J, T. Vladimirova and M.N. Sweeting (2009), Satellite Miniaturization Techniques
367 for Space Sensor Networks, *Journal of Spacecraft and Rockets*, Vol 46, No. 2, doi
368 10.2514/1.41639.

369 Daley, R. (1991), *Atmospheric Data Analysis*, Cambridge University Press, Cambridge, UK.

370 De la Beaujardiere, O. (2004), *C/NOFS: a Mission to Forecast Scintillations*, *Journal of*
371 *Atmospheric and Solar-Terrestrial Physics*, Vol. 66, No. 17, pp. 1573–1591.

372 Dyrud, L. P., Fentzke, J. T., Cahoy, K., Murphy, S., Wiscombe, W., Fish, C., Gunter, B., Bishop,
373 R., Bust, G., Erlandson, R., Bauer, B., & Gupta, O. (2012), *GEOScan: a geoscience facility from*
374 *space*. In *SPIE Defense, Security, and Sensing* (pp. 83850V-83850V). International Society for
375 Optics and Photonics.

376 Enloe, C. L., J. Lloyd, S. Meassick, C. Chan, J. O. McGarity, A. Huber, and P. Hartnett (1995),
377 *Compact Thermal Ion Detector for Space and Laboratory Applications*, *Review of Scientific*
378 *Instruments* 66.8, 4174-719.

379 Enloe, C. L., L. Habash Krause, R. K. Haaland, T. T. Patterson, C. E. Richardson, C. C. Lazidis,
380 and R. G. Whiting (2002), *Miniaturized electrostatic analyzer manufactured using*
381 *photolithographic etching*, *Review of Scientific Instruments* 74:3, DOI: 10.1063/1.1540715.

382 Evensen, G. (2003), *The Ensemble Kalman Filter: Theoretical Formulation and Practical*
383 *Implementation*, *Ocean Dynamics*, 53, 343–367, DOI 10.1007/s10236-003-0036-9.

384 Hajj, G. A., C. O. Ao, B. A. Iijima, D. Kuang, E. R. Kursinski, A. J. Mannucci, T. K. Meehan, L.
385 J. Romans, M. de la Torre Juarez, and T. P. Yunck (2004), *CHAMP and SAC-C atmospheric*
386 *occultation results and intercomparisons*, *J. Geophys. Res.*, 109, D06109,
387 doi:10.1029/2003JD003909.

388 Jenkins, P., R.J. Walters, M. J. Krasowski, J. J. Chapman, P. G. Ballard, J. A. Vasquez, D. R.
389 Mahoney, S. N. LaCava, W. R. Braun, N. F. Prokop, J. M. Flatico, L. C. Greer, K. B. Gibson,
390 W.H. Kinard, and H. G. Pippin (2009), MISSE-7: Building a Permanent Environmental Testbed
391 for the International Space Station, Proceedings of the 9th International Space Conference
392 Protection of Materials and Structures From Space Environment, Toronto, Canada, 19-23 May
393 2008, Ed. J.I. Kleiman, AIP Conference Proceedings 1087, pp. 273-276.

394 Kalman, A., A. Reif, D. Berkenstock, J. Mann and J. Cutler (2008), MISC - A Novel Approach
395 to Low-Cost Imaging Satellites, Proceedings of the 22nd Annual Conference On Small Satellites.

396 Kalman, A., A. Reif, and J. Martin (2013), MISC 3 – The next generation of 3U CubeSats,
397 Proceedings of the CubeSat Developers Summer Workshop.

398 Rocken, C., Y.H. You, W.S. Schreiner, D. Hunt, S. Sokolovskiy, and C. McCormick (2000),
399 COSMIC system description, *Terrestrial Atmospheric and Oceanic Sciences*, 11, 1, pp 21-52.

400 Scherliess, L., R.W. Schunk, J.J. Sojka, and D. Thompson (2004), Development of a Physics-
401 Based Reduced State Kalman Filter for the Ionosphere, *Radio Sci.*, 39, RS1S04,
402 doi:10.1029/2002RS002797.

403 Scherliess, L. D. Thompson, R.W. Schunk, and J.J. Sojka (2006), Ionospheric/thermospheric
404 variability at middle latitudes obtained from the global assimilation of ionospheric measurements
405 (GAIM) model, *Eos Trans. AGU*, 87(52), Fall Meet. Suppl., Abstract SA12A-03.

406 Scherliess, L., D.C. Thompson, and R.W. Schunk (2009), Ionospheric dynamics and drivers
407 obtained from a physics-based data assimilation model, *Radio Science*, **44**, RS0A32, doi:
408 10.1029/2008RS004068.

409 Scherliess, L., D.C. Thompson, and R.W. Schunk (2011), Data assimilation models: A 'new'
410 tool for ionosphere science and applications, in *The Dynamic Magnetosphere*, Springer, doi
411 10.1007/978-94-007-0501-2_18.

412 Schunk, R.W., L. Scherliess, J.J. Sojka, and D. Thompson (2004), Global Assimilation of
413 Ionospheric Measurements (GAIM), *Radio Sci*, **39**, RS1S02, doi:10.1029/2002RS002794.

414 Schunk, R.W., L. Scherliess, J.J. Sojka, D. Thompson, and L. Zhu (2005), Ionospheric Weather
415 Forecasting on the Horizon, *Space Weather*, **3**, S08007, doi:10.1029/2004SW000138.

416 Seo, J (2010), Overcoming Ionospheric Scintillation for Worldwide GPS Aviation, PhD thesis,
417 Stanford University, CA.

418 Straus, P. R., P. C. Anderson, and J. E. Danaher (2003), GPS occultation sensor observations of
419 ionospheric scintillation, *Geophys. Res. Lett.*, **30**, 1436, doi:10.1029/2002GL016503, 8.

420 Vladimirova, T., N. P. Bannister, J. Fothergill, G. W. Fraser, M. Lester, D. M. Wright, M. J.
421 Pont, D. J. Barnhart, O. Emam (2011), CubeSat Mission for Space Weather Monitoring,
422 Proceedings of 11th Australian Space Science Conference, ASSC'11, Canberra, Australia.

423 Wertz, J.R. (2006), Orbit and Constellation Design, in *Space Mission Analysis And Design*,
424 edited by W.J. Larson and J.R. Wertz, Microcosm Press, El Segundo, CA and Springer, New
425 York, NY.

426 **Figures**

Formatted: Don't keep with next

427 Figure 1: Geographical distribution of ground-based GPS-TEC observations chosen for this
428 study. The figure shows the 300 km pierce points of observations at the given time (2010/073
429 1200 UT), and the color scale depicts vertical TEC with blue indicating low TEC and red
430 indicating high TEC.

431

432 Figure 2: (upper panel) 25/5/1 Walker constellation ground tracks showing sampling of Ne from
433 "truth" model run, and (lower panel) snapshot of Ne obtained from an "improved ionospheric
434 specification" forecast model (GPS-TEC and sampled MESA data).

435

436 Figure 3: Model deviations from "truth" run for scenarios A and B, over the altitude-latitude
437 slice at longitude 161.25° E. Changes in Ne are denoted by variations in the color scale from
438 green (no deviation).

439

440 Figure 4: Snapshot of hmF2 for the "Truth" model.

441

442 Figure 5: Snapshot of hmF2 for the "ionospheric specification" model assimilating only GPS-
443 TEC into the GAIM-FP model.

444

445 Figure 6: Snapshot of hmF2 for the "improved ionospheric specification" model assimilating
446 GPS-TEC and in-situ MESA data into GAIM-FP.

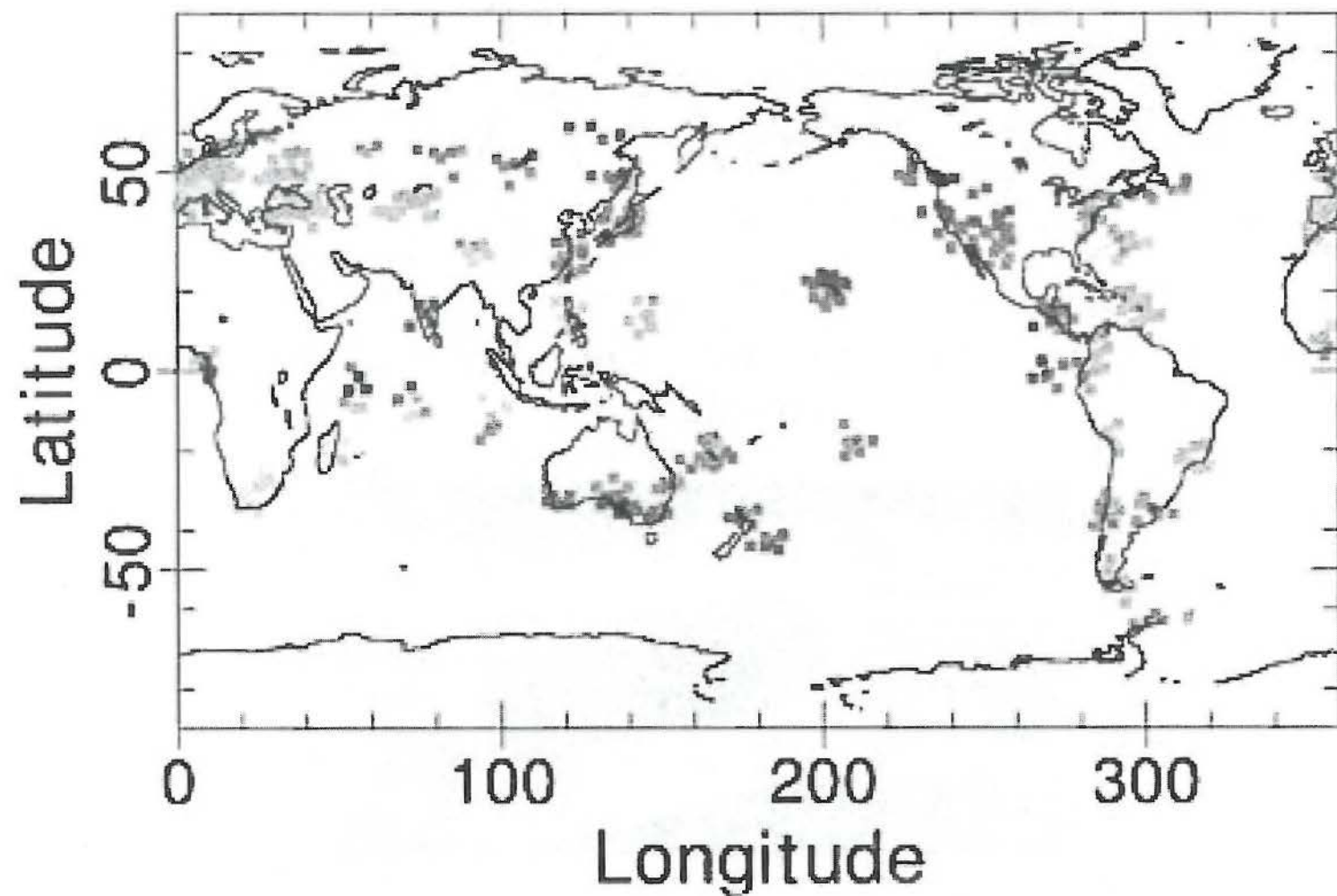
447

448 Figure 7: RMS deviation of hmF2 prediction (global sum). The upper (dotted) line shows
449 predictions from the "ionospheric specification" (GPS-TEC only); the lower (solid) plot shows
450 the predictions for "improved ionospheric specification" (GPS-TEC and MESA inputs).

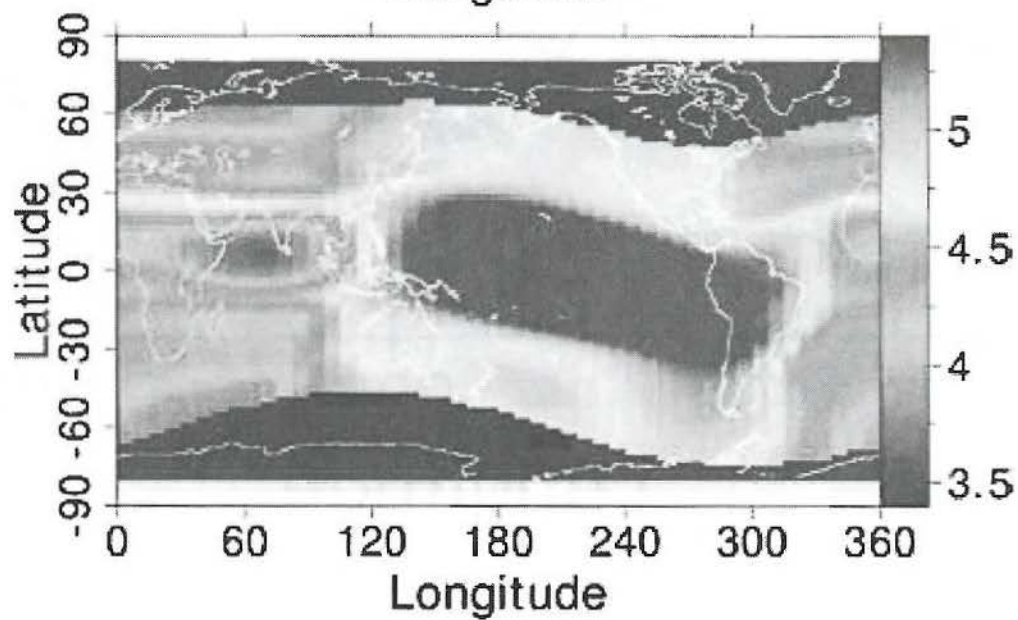
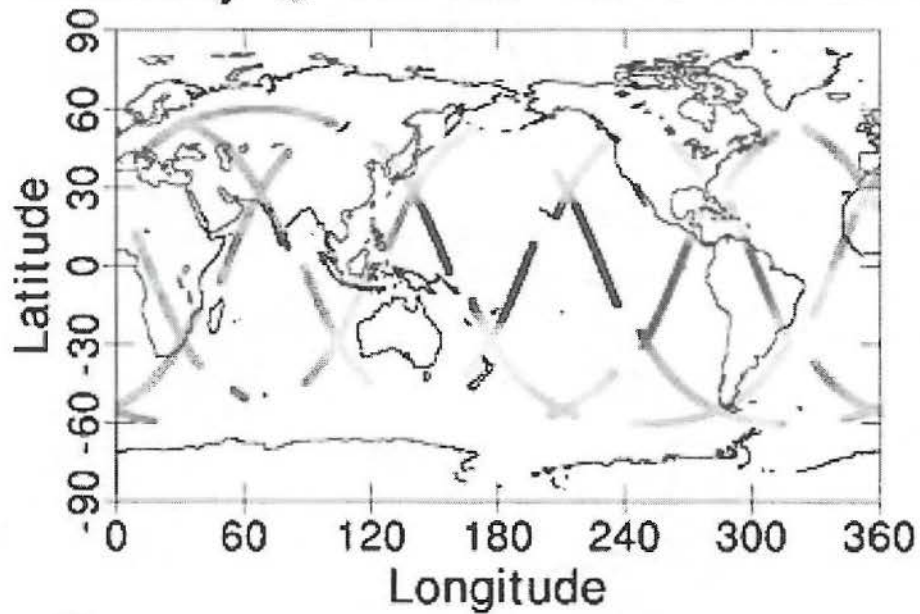
451

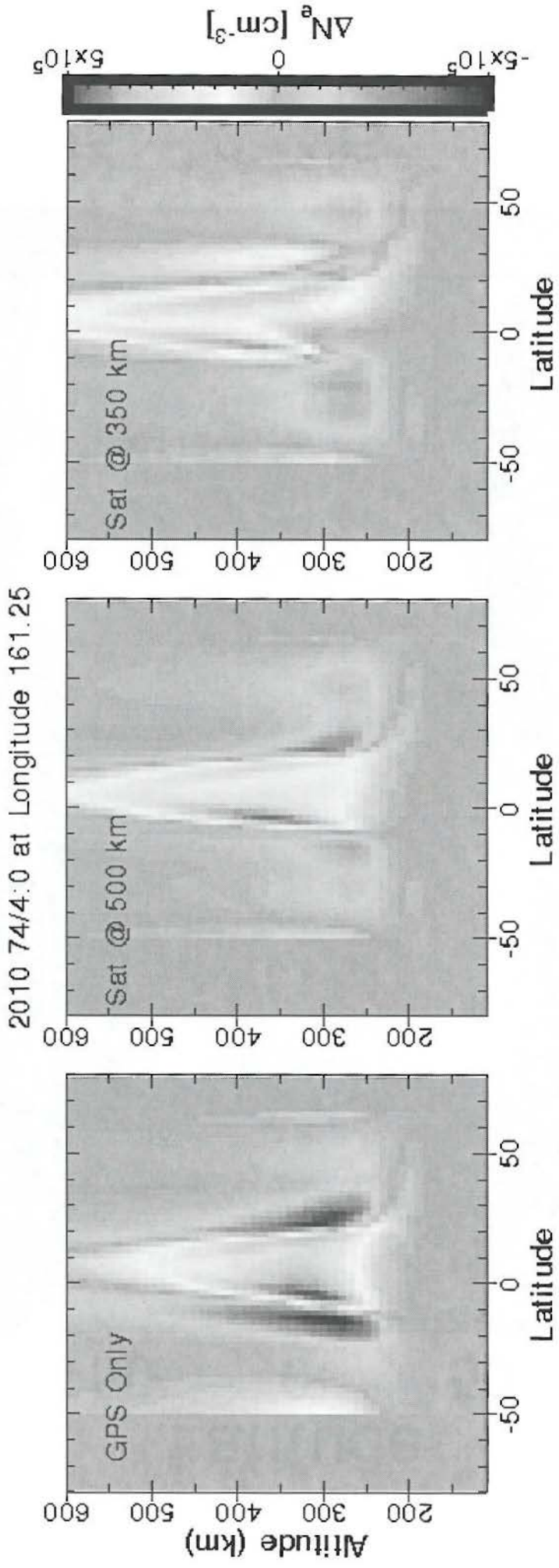
452 Figure 8: Skill Score of hmF2 prediction, comparing "improved ionospheric specification" to
453 "ionospheric specification".

TEC 2010 073/12:00 En: 01

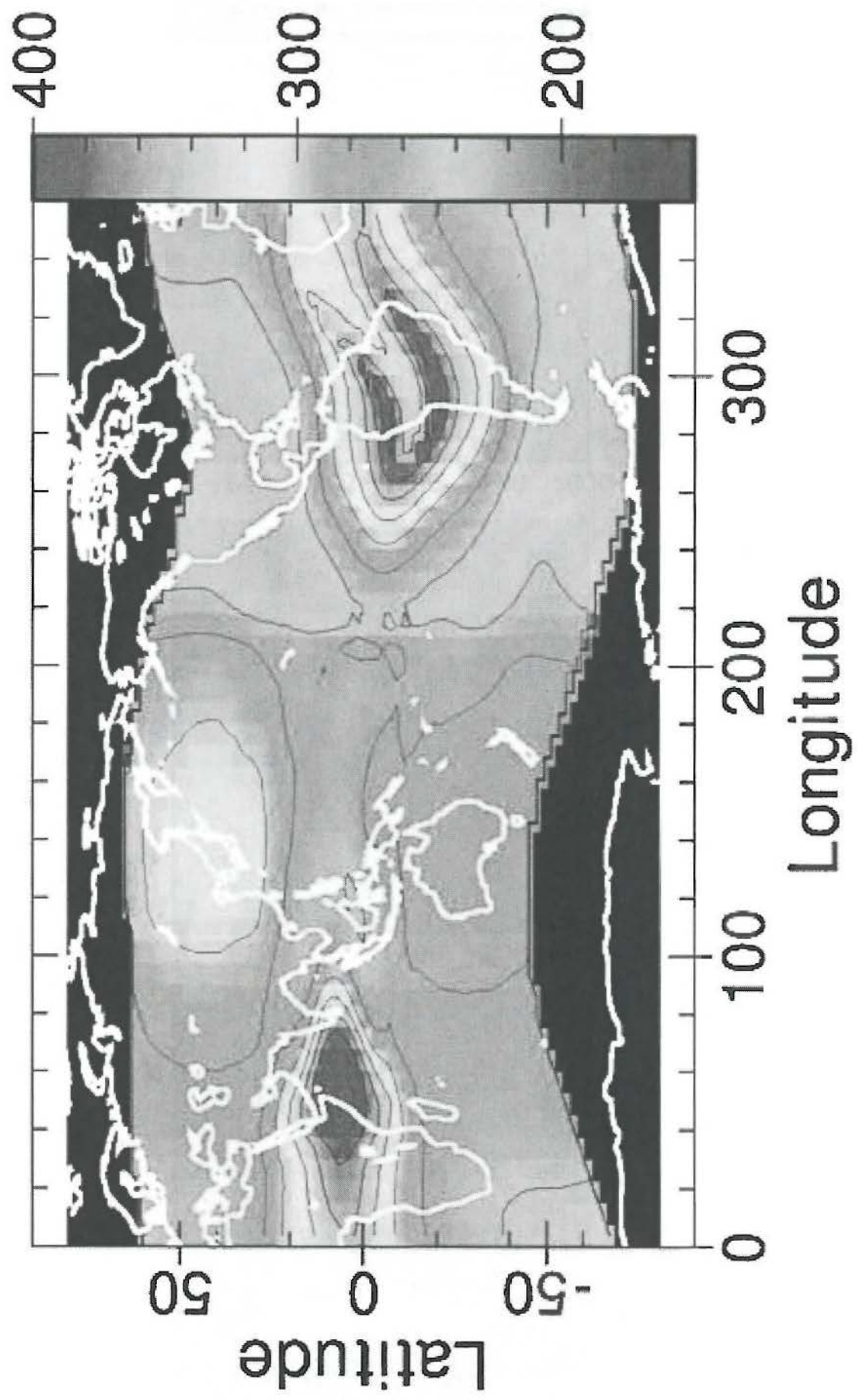


Edensity @ 510 km 2010 073/00:00

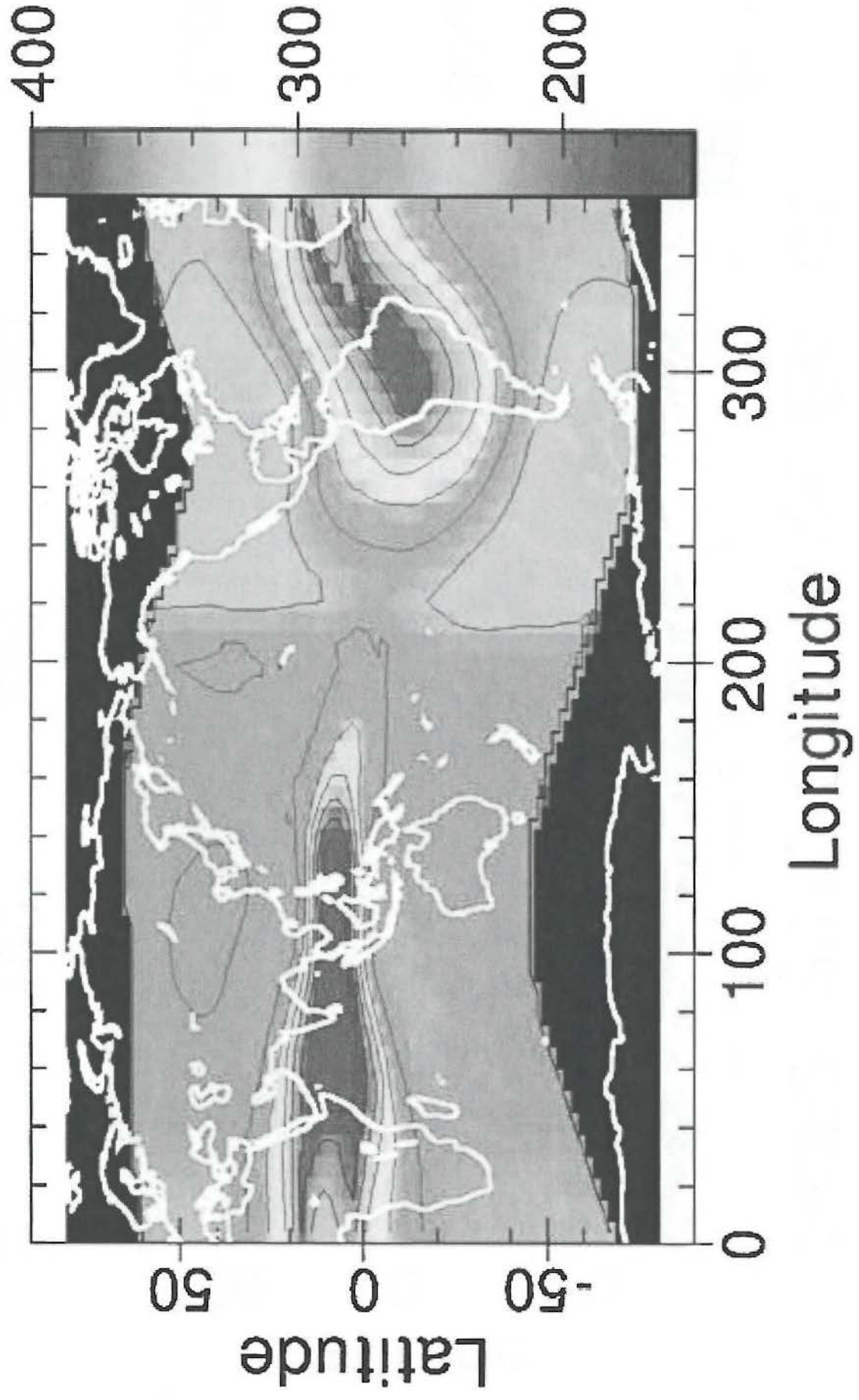




HMF2 2010 073/16:00 En: 00



HMF2 2010 073/16:00 En: 01



HMF2 2010 073/16:00 En: 01

